Available online at www.sciencedirect.com
ScienceDirect
Journal of Sound and Vibration 315 (2008) 1086–1102
JOURNAL OF SOUND AND VIBRATION
www.elsevier.com/locate/jsvi

In-plane vibrational analysis of rotating curved beam with elastically restrained root

Sen-Yung Lee[a,*], Jer-Jia Sheu[b], Shueei-Muh Lin[c]

[a]*National Cheng Kung University, Tainan, Taiwan 701, ROC*
[b]*Southern Taiwan University of technology, Tainan, Taiwan 710, ROC*
[c]*Kun Shan University, Tainan, Taiwan 710-03, ROC*

Received 5 November 2006; received in revised form 7 February 2008; accepted 10 February 2008
Handling Editor: L.G. Tham
Available online 8 April 2008

Abstract

This study analyzes the in-plane free vibration of a rotating curved beam with an elastically restrained root. Neglecting the effects of shear deformation and the Coriolis force, governing differential equations are derived for the coupled bending–extensional vibration of the curved beam using Hamilton's principle and a consistent linearization approach. Explicit relations are constructed to describe the correlation between the axial and radial displacements of the beam. These relations are then used to transform the coupled governing differential equations into a sixth-order ordinary differential equation expressed in terms of the radial displacement variable only. An exact closed-form fundamental solution of the transformed system is then derived. Finally, the respective effects of the arc angle, the rotational speed, the hub radius and the root spring constants on the natural frequencies and divergent instability characteristics of a curved rotating beam are systematically examined and compared with those observed for a straight cantilever beam.

1. Introduction

Rotating components are used in a wide variety of engineering applications, including vehicular propulsion systems, flexible rotating space booms, turbomachinery, automotive cooling systems, and so on. The dynamic behavior of such components is highly complex, and thus they are generally modeled in the form of a simple rotating beam. An excellent review of the vibrational characteristics of typical rotating components can be found in the studies presented by Leissa [1], Ramamurti and Balasubramanian [2], Rao [3], and Lin et al. [4].

Many researchers have employed approximation methods of various types to investigate the effects of the rotational speed, setting angle, material properties, pre-twist amount, shear deformation and rotary inertia on the bending vibrations of a straight rotating beam. For example, Ko [5] utilized the finite-difference technique to investigate the flexural behavior of tapered sandwich rotating beams, while Tomar [6] analyzed the effects of thermal gradients on the vibrational frequency of pretwisted rotating beams using the Rayleigh method.

*Corresponding author.
E-mail address: sylee@mail.ncku.edu.tw (S.-Y. Lee).

0022-460X/$ - see front matter © 2008 Elsevier Ltd. All rights reserved.
doi:10.1016/j.jsv.2008.02.011

Nagaraj and Shanthakumar [7] used the Galerkin finite element method to analyze rotor blade vibrations. Hodges and Rutkowski [8] analyzed the free vibrations of a rotating beam using a variable-order finite element method. Young and Lin [9] used a stochastic averaging technique to investigate the stability of rotating tapered pretwisted beams with randomly varying speeds. Hashemi et al. [10] proposed a new dynamic finite element method based on trigonometric shape functions for analyzing the vibrations of spinning beams. Banerjee [11] applied the dynamic stiffness method to analyze the free vibration of uniform and tapered straight beams.

In addition to the approximation methods described above, several researchers have also obtained exact solutions for the bending vibrations of rotating beams. For example, Storti and Aboelnaga [12] derived the exact solution for the bending vibrations of a class of rotating non-uniform beams with hyper-geometric solutions. Lee and Kuo [13,14] utilized a polynomial expansion technique to obtain the exact solution for the bending vibration of an elastically restrained rotating non-uniform beam. Lee and Lin [15] employed a numerical method to investigate the coupled effect of the rotational speed and the mass moment of inertia on the natural frequencies of a rotating non-uniform Timoshenko beam. Lin et al. [16] derived a semi-analytical steady-state solution for rotating beams with an elastically restrained root and investigated the effects of viscous damping on the natural frequency of the beam.

All of the studies reviewed above considered the beam to be perfectly straight. However, in practice, the performance of a fan is generally enhanced by curving the profile of the beams in either the forward or rearward direction [17]. Reviewing the literature, however, very little mention is found of the vibration characteristics of such beams due to the resulting complexity of the rotating system. Of those researchers which have investigated this problem, Wang and Mahrenholtz [18] used the Galerkin approximation method and the Legendre polynomial approach to investigate the effects of the hub radius, the cross-section orientation and the radius of curvature on the dynamic response of the rotating beam at various rotational speeds. However, the effect of the root stiffness was not considered. Park and Kim [19] conducted a dynamic analysis of a rotating curved beam with a tip mass using the finite element method. For simplicity, however, the effects of both the root stiffness and the hub radius were ignored.

In practice, the root stiffness of a rotating curved beam has a significant effect on its dynamic response and should therefore be taken into account. Accordingly, the current study applies Euler–Bernoulli beam theory and Hamilton's principle to derive two governing differential equations for the vibration of a rotating curved beam with an elastically restrained root in which both the root stiffness and the hub radius are taken into account. Explicit relations are constructed to correlate the radial and axial displacements of the beam and a closed-form solution of the rotating curved beam is then derived. Finally, the respective effects of the rotational speed, the arc angle, the hub radius and the root stiffness on the natural frequencies and divergent instability of the beam are systematically explored.

2. Derivation of motion equations

Consider a rotating curved beam with an elastically restrained root mounted in a hub with a radius of r_h and rotating with a constant angular speed Ω, as shown in Fig. 1. In accordance with Euler–Bernoulli theory, the radial cross-section of the beam is assumed to retain a planar form following its bending and axial deformation. Furthermore, an assumption is made that the beam is both homogeneous and isotropic. In addition, the beam has a slender cross-section, i.e. its thickness (in the plane of rotation) is far smaller than its width or radius of curvature. As a result, the beam deforms only in the plane of rotation. The vibration of the curved beam comprises an axial extension component and a bending deformation component. Neglecting the effect of shear deformation, the normal strain can be expressed as [15,20]

$$\varepsilon = \frac{\partial u}{\partial s} + \frac{v}{R} - r\left(\frac{\partial^2 v}{\partial s^2} - \frac{1}{R}\frac{\partial u}{\partial s}\right) + \frac{1}{2}\left(\frac{\partial v}{\partial s}\right)^2, \tag{1}$$

where u and v are the axial and radial displacements of the beam centroid, respectively, s denotes the axial coordinate, r is the distance from the centroidal axis, and R is the radius of curvature of the beam. Note that the nonlinear term in Eq. (1) is required to explain the influence of centrifugal force on the bending stiffness.

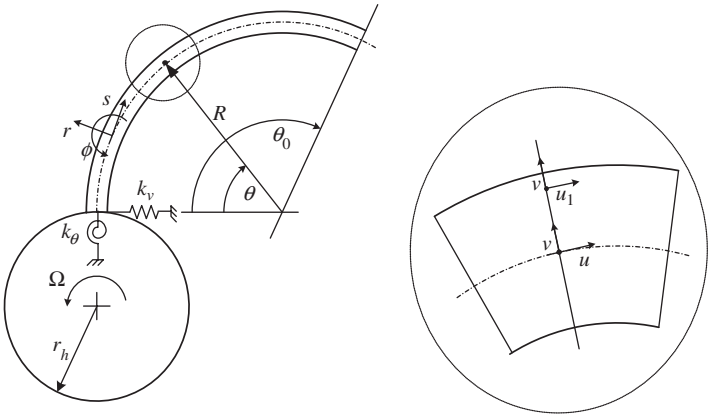

Fig. 1. Geometry and coordinate system of rotating curved beam with elastically restrained root.

The strain energy within the beam is given by

$$U = \frac{1}{2}\iint E\varepsilon^2 \,\mathrm{d}A\,\mathrm{d}s = \frac{1}{2}\iint E\left[\left(\frac{\partial u}{\partial s}+\frac{v}{R}\right) - r\left(\frac{\partial^2 v}{\partial s^2}-\frac{1}{R}\frac{\partial u}{\partial s}\right)+\frac{1}{2}\left(\frac{\partial v}{\partial s}\right)^2\right]^2 \mathrm{d}A\,\mathrm{d}s, \tag{2}$$

where E is Young's modulus and A is the cross-sectional area.

In Eq. (2), it is assumed that the rigidity of the beam in the radial direction is far lower than that in the axial direction. Moreover, an assumption is made that the deformation of the beam is relatively small. Therefore, applying the consistent linearization approach [21], the strain energy can be approximated as

$$U \cong \frac{1}{2}\int EA\left(\frac{\partial u}{\partial s}+\frac{v}{R}\right)^2 \mathrm{d}s + \frac{1}{2}\int EI\left(\frac{\partial^2 v}{\partial s^2}-\frac{1}{R}\frac{\partial u}{\partial s}\right)^2 \mathrm{d}s + \frac{1}{2}\int N_p\left(\frac{\partial v}{\partial s}\right)^2 \mathrm{d}s, \tag{3}$$

where I is the area moment of inertia and N_p is the axial centrifugal force acting on the undeformed rotating curved beam, and can be computed directly as

$$N_p = \rho AR\Omega^2[(\theta_0-\theta)(R\sin\theta + r_h\cos\theta) + R(1-\cos(\theta_0-\theta))], \tag{4}$$

where ρ is the mass density, θ_0 is the arc angle and θ is the angular coordinate.

If the hub is assumed to have zero radius, i.e. $r_h = 0$, Eq. (4) reduces to the form given by Park and Kim [19]. From Eq. (3), it can be seen that the strain energy comprises three components, namely the axial extension and bending deformation (shown in the first and second terms, respectively) and the rotation-induced axial centrifugal force.

Taking the stored energy induced by the root stiffness into account, the total potential energy within the beam system is given by

$$U_s = U + \tfrac{1}{2}k_v v(0,t)^2 + \tfrac{1}{2}k_\theta \phi(0,t)^2, \tag{5}$$

where k_v and k_θ represent the translational and rotational spring constants of the blade root, respectively, and ϕ is the rotational angle of the curved beam. Meanwhile, the kinetic energy of the rotating curved beam can be expressed as

$$T = \frac{1}{2}\int_0^{\theta_0} \rho AR(\overrightarrow{v_p}\cdot\overrightarrow{v_p})\,\mathrm{d}\theta, \tag{6}$$

where $\vec{v}_p$ is the absolute velocity of any arbitrary point p on the beam. It can be shown that the velocity has the form

$$\vec{v}_p = \left[\frac{\partial u}{\partial t} - \Omega(r_h\sin\theta + R(1-\cos\theta)+v)\right]\vec{e}_\theta + \left[\frac{\partial v}{\partial t}+\Omega(R\sin\theta + r_h\cos\theta + u)\right]\vec{e}_r, \tag{7}$$

where $\vec{e}_\theta$ and $\vec{e}_r$ are the axial and radial unit vectors, respectively. Utilizing the Hamilton principle, the variation of the total energy within the rotating curved beam can be expressed as

$$\int \delta(T - U_s)\,\mathrm{d}t = 0. \tag{8}$$

Thus, the following governing equations can be obtained:

$$\begin{aligned}&\frac{\partial Q}{\partial s} - \frac{N}{R} + \frac{\partial}{\partial s}\left(N_p \frac{\partial v}{\partial s}\right) - \rho A \frac{\partial^2 v}{\partial t^2} + \rho A \Omega^2 v - 2\rho A \Omega \frac{\partial u}{\partial t} \\ &= -\rho A \Omega^2 [r_h \sin\theta + R(1 - \cos\theta)],\end{aligned} \tag{9}$$

$$\frac{Q}{R} + \frac{\partial N}{\partial s} - \rho A \frac{\partial^2 u}{\partial t^2} + \rho A \Omega^2 u + 2\rho A \Omega \frac{\partial v}{\partial t} = -\rho A \Omega^2 (R \sin\theta + r_h \cos\theta) \tag{10}$$

with boundary conditions of

at $s = 0$:

$$u = 0, \tag{11a}$$

$$Q + N_p \frac{\partial v}{\partial s} - k_v v = 0, \tag{11b}$$

$$M - k_\theta \phi = 0 \tag{11c}$$

and

at $s = L$:

$$N = 0, \tag{12a}$$

$$Q = 0, \tag{12b}$$

$$M = 0. \tag{12c}$$

Note that the beam length, L, is given by $L = R\theta_0$. In Eqs. (12a)–(12c), N, Q and M represent the axial normal force, the shear force and the bending moment, respectively, and are given by

$$N = EA\left(\frac{\partial u}{\partial s} + \frac{v}{R}\right),\ Q = -EI\left(\frac{\partial^3 v}{\partial s^3} - \frac{1}{R}\frac{\partial^2 u}{\partial s^2}\right) \text{ and } M = EI\left(\frac{\partial^2 v}{\partial s^2} - \frac{1}{R}\frac{\partial u}{\partial s}\right). \tag{13}$$

It can be seen that Eqs. (9) and (10) both contain a static centrifugal force component. For a straight beam, $\theta_0 = 0$, no static centrifugal force is induced along the radial direction. Furthermore, for a non-rotating curved beam, the two governing equations have the same forms as those given by Henrych [22].

3. Free vibration of rotating curved beam and solution procedure

3.1. Rotating curved beam

The axial and radial displacements of the rotating curved beam comprise both dynamic and static components, i.e. $u = u_d + u_s$ and $u = v_d + v_s$, respectively, where u_d and u_s are the dynamic and static displacements of the beam centroid in the axial direction, while v_d and v_s are the dynamic and static displacements of the beam centroid in the radial direction. As a result, the rotating beam system can be divided into two subsystems, namely a dynamic system and a static system. The governing differential equations of the dynamic subsystem can be expressed as

$$\frac{\partial Q_d}{\partial s} - \frac{N_d}{R} + \frac{\partial}{\partial s}\left(N_p \frac{\partial v_d}{\partial s}\right) - \rho A \frac{\partial^2 v_d}{\partial t^2} + \rho A \Omega^2 v_d - 2\rho A \Omega \frac{\partial u_d}{\partial t} = 0, \tag{14}$$

$$\frac{Q_d}{R}+\frac{\partial N_d}{\partial s}-\rho A\frac{\partial^2 u_d}{\partial t^2}+\rho A\Omega^2 u_d+2\rho A\Omega\frac{\partial v_d}{\partial t}=0. \tag{15}$$

The corresponding boundary conditions have the form
at $s=0$:

$$u_d=0, \tag{16a}$$

$$Q_d+N_p\frac{\partial v_d}{\partial s}-k_v v_d=0, \tag{16b}$$

$$M_d-k_\theta\phi_d=0 \tag{16c}$$

and
at $s=L$

$$N_d=0, \tag{17a}$$

$$Q_d=0, \tag{17b}$$

$$M_d=0, \tag{17c}$$

where M_d, N_d, Q_d and ϕ_d are defined respectively as

$$M_d=EI\left(\frac{\partial^2 v_d}{\partial s^2}-\frac{1}{R}\frac{\partial u_d}{\partial s}\right),\ N_d=EA\left(\frac{\partial u_d}{\partial s}+\frac{v_d}{R}\right),$$
$$Q_d=-EI\left(\frac{\partial^3 v_d}{\partial s^3}-\frac{1}{R}\frac{\partial^2 u_d}{\partial s^2}\right)\text{ and }\phi_d=\frac{\partial v_d}{\partial s}-\frac{u_d}{R}.$$

It is well known that at low rotational speeds, the Coriolis force has a negligible effect on the dynamic response of a beam with a large slenderness ratio. In the current analysis, it is assumed that the curved beam has a sufficiently large slenderness ratio that the Coriolis force can be ignored.

3.2. Dimensionless governing equations

Assuming that the rotating curved beam exhibits time-harmonic vibration with an angular frequency ω, its dynamic displacements in the radial and axial directions can be expressed as

$$v_d(s,t)=\tilde{V}(s)\,e^{i\omega t}\text{ and }u_d(s,t)=\tilde{U}(s)\,e^{i\omega t}. \tag{18}$$

For analytical convenience, the following dimensionless parameters are introduced:

$$L_z=L\sqrt{\frac{A}{I}},\quad \overline{N_p}=\frac{N_p}{\rho A\Omega^2L^2},\quad \bar{V}=\frac{\tilde{V}}{L},\quad \bar{U}=\frac{\tilde{U}}{L},\quad \alpha=\sqrt{\frac{\rho A}{EI}}\Omega L^2,\quad \beta_v=\frac{k_vL^3}{EI},\quad \beta_\theta=\frac{k_\theta L}{EI},$$
$$\mu=\frac{r_h}{L},\quad \xi=\frac{s}{L},\quad \Lambda=\sqrt{\frac{\rho A}{EI}}\omega L^2. \tag{19}$$

The coupled differential equations given in Eqs. (14) and (15) can then be rewritten in the following non-dimensional form:

$$\left(\bar{V}^{(4)}-\theta_0\bar{U}'''\right)+L_z^2\theta_0(\bar{U}'+\theta_0\bar{V})-\alpha^2(\bar{N}_p\bar{V}')'-(\Lambda^2+\alpha^2)\bar{V}=0, \tag{20}$$

$$(\bar{V}'''-\theta_0\bar{U}'')-\frac{L_z^2}{\theta_0}(\bar{U}''+\theta_0\bar{V}')-\frac{1}{\theta_0}(\Lambda^2+\alpha^2)\bar{U}=0, \tag{21}$$

where the prime symbol indicates differentiation with respect to the dimensionless variable ξ. The corresponding dimensionless boundary conditions are given by

at $\xi = 0$:

$$\bar{U} = 0, \tag{22a}$$

$$\bar{V}''' - \theta_0 \bar{U}'' - \alpha^2 \bar{N}_p \bar{V}' + \beta_v \bar{V} = 0, \tag{22b}$$

$$\bar{V}'' - \theta_0 \bar{U}' - \beta_\theta(\bar{V}' - \theta_0 \bar{U}) = 0, \tag{22c}$$

at $\xi = 1$:

$$\bar{U}' + \theta_0 \bar{V} = 0, \tag{23a}$$

$$\bar{V}''' - \theta_0 \bar{U}'' = 0, \tag{23b}$$

$$\bar{V}'' - \theta_0 \bar{U}' = 0, \tag{23c}$$

where the dimensionless axial centrifugal force has the form

$$\bar{N}_p = \frac{1}{\theta_0^2}[\theta_0(1-\xi)(\sin(\theta_0\xi) + \mu\theta_0 \cos(\theta_0\xi)) + (1 - \cos(\theta_0 - \theta_0\xi))]. \tag{24}$$

3.3. Displacement relations and decoupling of governing equations

Multiplying Eq. (20) by a factor $(\theta_0 + L_z^2/\theta_0)$, multiplying the derivative of Eq. (21) by θ_0 and then subtracting the former from the latter, the following displacement relation is obtained:

$$\bar{U}' = \frac{1}{k_6}\left[k_7 \bar{V} + k_8 \bar{N}_p' \bar{V}' + (k_8 \bar{N}_p - \theta_0 L_z^2)\bar{V}'' - \frac{L_z^2}{\theta_0}\bar{V}^{(4)}\right]. \tag{25a}$$

Substituting the derivative of Eq. (25a) back into Eq. (21) yields the following relation:

$$\bar{U} = \frac{1}{k_1}\left[(k_2 + k_3 \bar{N}_p'')\bar{V}' + 2k_3 \bar{N}_p' \bar{V}'' + (k_3 \bar{N}_p + k_4)\bar{V}''' + k_5 \bar{V}^{(5)}\right]. \tag{25b}$$

Finally, substituting Eqs. (25a) and (25b) back into Eq. (21) yields

$$\bar{U}'' = \frac{k_8}{k_3 k_6}[(k_2 + k_3 \bar{N}_p'' + k_6 L_z^2)\bar{V}' + 2k_3 \bar{N}_p \bar{V}'' + (k_3 \bar{N}_p + k_4 - k_6)\bar{V}''' + k_5 \bar{V}^{(5)}]. \tag{25c}$$

Note that the coefficients k_i in Eqs. (25a)–(25c) are listed in Appendix A. Substituting Eq. (25a) and the derivative of Eq. (25c) back into Eq. (20), a sixth-order differential equation is obtained in terms of the variable $\bar{V}$ only, i.e.

$$\bar{V}^{(6)} + a_4 \bar{V}^{(4)} + a_3 \bar{V}''' + a_2 \bar{V}'' + a_1 \bar{V}' + a_0 \bar{V} = 0, \tag{26}$$

where

$$\begin{aligned}
a_0 &= -\frac{(\Lambda^2 + \alpha^2)^2}{L_z^2} + \theta_0^2(\Lambda^2 + \alpha^2), \quad a_1 = -\frac{\alpha^2}{L_z^2}(\Lambda^2 + \alpha^2)\bar{N}_p' - \alpha^2\left(1 + \frac{\theta_0^2}{L_z^2}\right)\bar{N}_p''', \\
a_2 &= -(\Lambda^2 + \alpha^2)\left(1 + \frac{\theta_0^2}{L_z^2}\right) + \theta_0^4 - \frac{\alpha^2}{L_z^2}(\Lambda^2 + \alpha^2)\bar{N}_p - 3\alpha^2\left(1 + \frac{\theta_0^2}{L_z^2}\right)\bar{N}p'', \\
a_3 &= -3\alpha^2\left(1 + \frac{\theta_0^2}{L_z^2}\right)\bar{N}_p', \quad a_4 = \frac{(\Lambda^2 + \alpha^2)}{L_z^2} + 2\theta_0^2 - \alpha^2\left(1 + \frac{\theta_0^2}{L_z^2}\right)\bar{N}_p.
\end{aligned} \tag{27}$$

Meanwhile, substituting the relations given in Eq. (25) into Eqs. (22) and (23), the boundary conditions in terms of $\bar{V}$ only are obtained as follows:

At $\xi = 0$:

$$b_{16}\bar{V}^{(5)} + b_{15}\bar{V}^{(4)} + b_{14}\bar{V}''' + b_{13}\bar{V}'' + b_{12}\bar{V}' + b_{11}\bar{V} = 0, \tag{28a}$$

$$b_{26}\bar{V}^{(5)} + b_{25}\bar{V}^{(4)} + b_{24}\bar{V}''' + b_{23}\bar{V}'' + b_{22}\bar{V}' + b_{21}\bar{V} = 0, \tag{28b}$$

$$b_{36}\bar{V}^{(5)} + b_{35}\bar{V}^{(4)} + b_{34}\bar{V}''' + b_{33}\bar{V}'' + b_{32}\bar{V}' + b_{31}\bar{V} = 0, \tag{28c}$$

At $\xi = 0$:

$$b_{46}\bar{V}^{(5)} + b_{45}\bar{V}^{(4)} + b_{44}\bar{V}''' + b_{43}\bar{V}'' + b_{42}\bar{V}' + b_{41}\bar{V} = 0, \tag{29a}$$

$$b_{56}\bar{V}^{(5)} + b_{55}\bar{V}^{(4)} + b_{54}\bar{V}''' + b_{53}\bar{V}'' + b_{52}\bar{V}' + b_{51}\bar{V} = 0, \tag{29b}$$

$$b_{66}\bar{V}^{(5)} + b_{65}\bar{V}^{(4)} + b_{64}\bar{V}''' + b_{63}\bar{V}'' + b_{62}\bar{V}' + b_{61}\bar{V} = 0. \tag{29c}$$

Note that the coefficients b_{ij} in Eqs. (28) and (29) are presented in Appendix B.

Collectively, Eqs. (26)–(29) provide a complete description of the dynamic response of the rotating curved beam system in terms of the radial displacement only.

4. Fundamental solutions and frequency equation

The decoupled governing differential equation given in Eq. (26) is a sixth-order ordinary differential equation with variable coefficients. In general, the exact fundamental solutions for equations of this form cannot be easily obtained. However, if the coefficients of the differential equation can be expressed in the following polynomial form:

$$a_0 = \sum_{i=0}^{n0} d_i\xi^i, \quad a_1 = \sum_{i=0}^{n1} e_i\xi^i, \quad a_2 = \sum_{i=0}^{n2} f_i\xi^i, \quad a_3 = \sum_{i=0}^{n3} g_i\xi^i, \quad a_4 = \sum_{i=0}^{n4} h_i\xi^i, \tag{30}$$

then the six linearly independent fundamental solutions, $w_i(\xi)$, $i = 1$–6, of Eq. (26) which satisfy the following normalization condition at the origin of the coordinate system

$$\begin{bmatrix} w_1(0) & w_2(0) & w_3(0) & w_4(0) & w_5(0) & w_6(0) \\ w_1'(0) & w_2'(0) & w_3'(0) & w_4'(0) & w_5'(0) & w_6'(0) \\ w_1''(0) & w_2''(0) & w_3''(0) & w_4''(0) & w_5''(0) & w_6''(0) \\ w_1'''(0) & w_2'''(0) & w_3'''(0) & w_4'''(0) & w_5'''(0) & w_6'''(0) \\ w_1^{(4)}(0) & w_2^{(4)}(0) & w_3^{(4)}(0) & w_4^{(4)}(0) & w_5^{(4)}(0) & w_6^{(4)}(0) \\ w_1^{(5)}(0) & w_2^{(5)}(0) & w_3^{(5)}(0) & w_4^{(5)}(0) & w_5^{(5)}(0) & w_6^{(5)}(0) \end{bmatrix} = \begin{bmatrix} 1 & 0 & 0 & 0 & 0 & 0 \\ 0 & 1 & 0 & 0 & 0 & 0 \\ 0 & 0 & 1 & 0 & 0 & 0 \\ 0 & 0 & 0 & 1 & 0 & 0 \\ 0 & 0 & 0 & 0 & 1 & 0 \\ 0 & 0 & 0 & 0 & 0 & 1 \end{bmatrix} \tag{31}$$

can be obtained by extending the technique used by Lee and Kuo [14] and using the power series method originally applied by Stafford and Giurgiutiu [23,24]. Otherwise, approximated solutions can be obtained using the algorithm developed by Lee and Kuo [13].

The six linearly independent fundamental solutions are assumed to have the form

$$w_i(\xi) = \sum_{n=0}^{\infty} k_{i,n}\xi^n, \quad i = 1, 2, \ldots, 6, \tag{32a}$$

where

$$\begin{aligned}
&\text{for } w_1(\xi): k_{1,0} = 1, \quad k_{1,1} = k_{1,2} = k_{1,3} = k_{1,4} = k_{1,5} = 0,\\
&\text{for } w_2(\xi): k_{2,1} = 1, \quad k_{2,0} = k_{2,2} = k_{2,3} = k_{2,4} = k_{2,5} = 0,\\
&\text{for } w_3(\xi): k_{3,2} = 1/2, \quad k_{3,0} = k_{3,1} = k_{3,3} = k_{3,4} = k_{3,5} = 0,\\
&\text{for } w_4(\xi): k_{4,3} = 1/6, \quad k_{4,0} = k_{4,1} = k_{4,2} = k_{4,4} = k_{4,5} = 0,\\
&\text{for } w_5(\xi): k_{5,4} = 1/24, \quad k_{5,0} = k_{5,1} = k_{5,2} = k_{5,3} = k_{5,5} = 0,\\
&\text{for } w_6(\xi): k_{6,5} = 1/120, \quad k_{6,0} = k_{6,1} = k_{6,2} = k_{6,3} = k_{6,4} = 0.
\end{aligned} \tag{32b}$$

Substituting Eqs. (30), (32) into Eq. (26) and collecting the coefficients of those terms with like powers of ξ, the following recurrence formula can be obtained:

$$\begin{aligned}
k_{i,m+6} = \frac{-1}{(m+6)(m+5)\cdots(m+1)} \Bigg\{ &\left[\sum_{j=1}^{m}(m-j+6)\cdots(m-j+1)k_{i,m-j+6}\right]\\
&+\left[\sum_{j=0}^{m}(m-j+4)\cdots(m-j+1)h_j k_{i,m-i+4}\right]\\
&+\left[\sum_{j=0}^{m}(m-j+3)\cdots(m-j+1)g_j k_{i,m-j+3}\right]\\
&+\left[\sum_{j=0}^{m}(m-j+2)(m-j+1)f_j k_{i,m-j+2}\right]\\
&+\left[\sum_{j=0}^{m}(m-j+1)e_j k_{i,m-j+1}\right]+\left[\sum_{j=0}^{m} d_j k_{i,m-j}\right]\Bigg\}, \quad m = 0, 1, \cdots \to \infty.
\end{aligned} \tag{33}$$

This formula enables the six exact normalized fundamental solutions given in Eq. (32) to be generated. Thus, the general solution of the rotating beam system can be expressed as

$$\bar{V}(\xi) = \sum_{i=1}^{6} c_i w_i(\xi), \tag{34}$$

where c_i ($i = 1$–6) are constants whose values are to be determined.

Substituting the general solution given in Eq. (34) into the associated boundary conditions given in Eqs. (28a)–(29c) yields the following set of equations:

$$[B_{ij}]\{c_i\} = 0, \; i, j = 1 - 6, \tag{35}$$

where

$$B_{ij} = b_{ij}, \quad i = 1, 2, 3, \quad B_{ij} = \sum_{k=1}^{6} b_{ik} w_j^{(k-1)}(1), \quad i = 4, 5, 6, \quad j = 1, 2, \ldots, 6. \tag{36}$$

As a result, the natural frequencies of the rotating curved beam with an elastically restrained root can be derived from the following frequency equation:

$$|B_{ij}| = 0. \tag{37}$$

5. Rotating straight beam

For the case where the arc angle approaches a value of zero, the curved beam transforms into a straight beam and the coefficients given in Eq. (27) for the sixth-order differential displacement equation given in Eq. (26) become

$$a_0 = -\frac{(\Lambda^2+\alpha^2)^2}{L_z^2}, \quad a_1 = -\frac{\alpha^2}{L_z^2}(\Lambda^2+\alpha^2)\bar{N}_p' - \alpha^2\bar{N}_p''',$$
$$a_2 = -(\Lambda^2+\alpha^2) - \frac{\alpha^2}{L_z^2}(\Lambda^2+\alpha^2)\bar{N}_p - 3\alpha^2\bar{N}_p'', \quad a_3 = -3\alpha^2\bar{N}_p'$$
$$a_4 = \frac{(\Lambda^2+\alpha^2)}{L_z^2} - \alpha^2\bar{N}_p. \tag{38}$$

Eq. (26), with the coefficients given in Eq. (38), can then be expressed as

$$\left(D^2 + \frac{\Lambda^2+\alpha^2}{L_z^2}\right)(D^4 - \alpha^2\bar{N}_p D^2 - \alpha^2\bar{N}_p' D - \Lambda^2 - \alpha^2)\bar{V} = 0, \tag{39}$$

where D is the differentiation operator with respect to the dimensionless variable ξ. For a straight beam, Eq. (39) reduces to the following form:

$$(D^4 - \alpha^2\bar{N}_p D^2 - \alpha^2\bar{N}_p' D - \Lambda^2 - \alpha^2)\bar{V} = 0 \tag{40}$$

which is consistent with that given by Lee and Kuo [13]. Applying the procedure presented in Appendix C, it can be shown that the boundary conditions for the limiting case of a straight rotating beam have the form

at $\xi = 0$:

$$\bar{V}''' - \alpha^2\bar{N}_p\bar{V}' + \beta_v\bar{V} = 0, \tag{41a}$$

$$\bar{V}'' - \beta_\theta\bar{V}' = 0, \tag{41b}$$

at $\xi = 1$:

$$\bar{V}''' = 0, \tag{42a}$$

$$\bar{V}'' = 0. \tag{42b}$$

Alternatively, the limiting boundary conditions (Eqs. (41) and (42)) can be obtained simply by setting $\theta_0 = 0$ in the boundary conditions given in Eqs. (22) and (23).

6. Verification and discussion

To demonstrate the accuracy and efficiency of the proposed solution procedure, two examples are presented for illustration purposes. The first example considers the limiting case of a straight beam in which the radius of curvature $R \to \infty$ and the arc angle $\theta_0 \to 0$. Table 1 summarizes the results obtained for the natural frequencies (Λ) of the straight rotating beam at various values of the hub radius (μ) by the current method and by the methods presented by Yoo and Shin [25] and Putter and Mandor [26], respectively. It is evident that a good agreement is obtained between the three sets of results. Fig. 2 compares the results obtained using the proposed method for the fundamental natural frequencies of two curved cantilever beams with arc angles of $\theta_0 = 50^\circ$ and 90°, respectively, with those computed using the finite element method presented in Ref. [19]

Table 1
Comparison of results obtained for natural frequencies in chordwise bending vibration of straight cantilever beam

μ	α	Mode	Present	[25]	[26]
0	2	1	3.62	3.62	3.61
		2	22.5	22.5	22.5
	10	1	5.05	5.05	5.05
		2	32.1	32.1	32.1
1	2	1	4.40	4.40	4.40
		2	23.3	23.3	23.3
	10	1	13.3	13.3	13.3
		2	43.2	43.2	43.2
5	2	1	6.65	6.65	6.65
		2	26.1	26.1	26.1
	10	1	27.7	27.7	27.7
		2	71.4	71.4	71.4

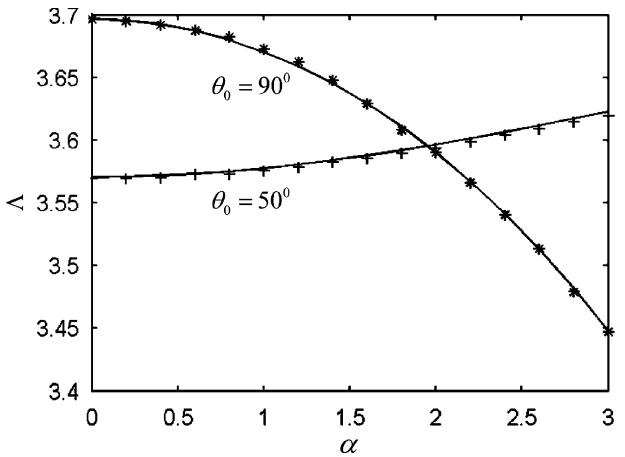

Fig. 2. Comparison of results obtained for fundamental natural frequencies of curved cantilever beams with arc angles of $\theta_0 = 50^\circ$ and 90°, respectively ($\mu = 0$ and $L_z = 100\sqrt{3}\theta_0$; solid line: present; symbol '*' and '+' [19]).

under equivalent conditions. Again, it is evident that a good agreement exists between the two sets of results in both cases.

Table 2 illustrates the influence of the rotational speed α and arc angle θ_0 on the first four natural frequencies of a curved cantilever beam with a slenderness ratio $L_z = 100$ mounted in a hub with a radius of $\mu = 0$. It can be seen that in the first vibrational mode, the fundamental natural frequency increases with an increasing rotational speed at an arc angle of $\theta_0 = 10^\circ$, increases and then decreases with an increasing rotational speed at an arc angle of $\theta_0 = 50^\circ$, and decreases continuously with an increasing rotational speed at an arc angle of $\theta_0 = 90^\circ$. Furthermore, comparing the results presented in Table 2 for the fundamental natural frequencies of the first vibrational mode with the corresponding results presented in Table 1, it can be seen that when the arc angle has a low value (i.e. $\theta_0 = 10^\circ$), the dynamic behavior of the curved beam is very similar to that of a straight beam since the resulting centrifugal force increases the rigidity of the beam. However, as the arc angle is increased, it is observed that the behavior of the rotating curved beam diverges markedly from that of the straight beam; particularly at higher values of the rotational speed. This result is to be expected since higher values of the arc angle θ_0 and rotational speed α lead to a greater centrifugal force, which in turn prompts a greater deformation of the beam in the first vibrational mode. In other words, the coupled effect of θ_0 and α reduces the bending rigidity of the beam in the first mode. The rightmost column of Table 2(a) shows

Table 2a
Influence of rotational speed α and arc angle θ_0 on first two natural frequencies of curved cantilever beam [$L_z = 100$, $\mu = 0$]

α	$\theta_0 = 10^\circ$		$\theta_0 = 50^\circ$		$\theta_0 = 90^\circ$	
	Λ_1	Λ_2	Λ_1	Λ_2	Λ_1	Λ_2
0.00	3.5182	21.9561	3.5707	20.3331	3.6965	17.7977
1.00	3.5445	22.0796	3.5777	20.4448	3.6704	17.8886
2.00	3.6205	22.4458	3.5966	20.7764	3.5900	18.1584
3.00	3.7381	23.0433	3.6230	21.3175	3.4478	18.5989
4.00	3.8871	23.8548	3.6501	22.0522	3.2304	19.1974
5.00	4.0570	24.8588	3.6711	22.9613	2.9141	19.9386
6.00	4.2392	26.0326	3.6795	24.0241	2.4530	20.8057
7.00	4.4274	27.3535	3.6697	25.2197	1.7249	21.7818
7.83	4.5847	28.5446	3.6444	26.2976	0	22.6623
8.00	4.6171	28.8001	3.6370	26.5286	–	22.8510
9.00	4.8054	30.3532	3.5771	27.9334	–	23.9989
10.0	4.9906	31.9963	3.4855	29.4186	–	25.2126

Table 2b
Influence of rotational speed α and arc angle θ_0 on third and fourth natural frequencies of curved cantilever beam [$L_z = 100$, $\mu = 0$]

α	$\theta_0 = 10^\circ$		$\theta_0 = 50^\circ$		$\theta_0 = 90^\circ$	
	Λ_3	Λ_4	Λ_3	Λ_4	Λ_3	Λ_4
0	61.6015	120.7387	59.5946	117.9619	56.0887	114.1167
1	61.7376	120.8828	59.7223	118.0964	56.2013	114.2390
2	62.1437	121.3140	60.1035	118.4985	56.5377	114.6047
3	62.8142	122.0288	60.7328	119.1647	57.0931	115.2110
4	63.7395	123.0212	61.6013	120.0892	57.8600	116.0528
5	64.9075	124.2835	62.6974	121.2638	58.8283	117.1235
6	66.3037	125.8060	64.0076	122.6787	59.9863	118.4148
7	67.9121	127.5773	65.5167	124.3222	61.3207	119.9173
8	69.7161	129.5849	67.2088	126.1812	62.8177	121.6200
9	71.6987	131.8153	69.0678	128.2413	64.4632	123.5116
10	73.8434	134.2537	71.0778	130.4868	66.2429	125.5799

Table 3a
Influence of rotational speed α and arc angle θ_0 on first two natural frequencies of curved cantilever beam [$L_z = 100$, $\mu = 1$]

α	$\theta_0 = 10^\circ$		$\theta_0 = 50^\circ$		$\theta_0 = 90^\circ$	
	Λ_1	Λ_2	Λ_1	Λ_2	Λ_1	Λ_2
0	3.5182	21.9561	3.5707	20.3331	3.6965	17.7977
1	3.7576	22.2725	3.7544	20.6100	3.7889	17.9996
2	4.3939	23.1949	4.2549	21.4179	4.0517	18.5899
3	5.2764	24.6530	4.9705	22.6962	4.4495	19.5273
4	6.2933	26.5546	5.8150	24.3652	4.9436	20.7562
5	7.3826	28.8071	6.7338	26.3437	5.5016	22.2181
6	8.5123	31.3293	7.6960	28.5601	6.1006	23.8601
7	9.6656	34.0564	8.6842	30.9565	6.7254	25.6380
8	10.8333	36.9386	9.6885	33.4879	7.3662	27.5169
9	12.0104	39.9385	10.7030	36.1205	8.0171	29.4701
10	13.1937	43.0289	11.7242	38.8291	8.6742	31.4775

Table 3b
Influence of rotational speed α and arc angle θ_0 on third and fourth natural frequencies of curved cantilever beam [$L_z = 100$, $\mu = 1$]

α	$\theta_0 = 10^\circ$		$\theta_0 = 50^\circ$		$\theta_0 = 90^\circ$	
	Λ_3	Λ_4	Λ_3	Λ_4	Λ_3	Λ_4
0	61.6015	120.7387	59.5946	117.9619	56.0887	114.1167
1	61.9378	121.0936	59.8999	118.2837	56.3353	114.3895
2	62.9344	122.1509	60.8048	119.2418	57.0665	115.2024
3	64.5559	123.8889	62.2775	120.8149	58.2578	116.5387
4	66.7494	126.2730	64.2701	122.9690	59.8720	118.3722
5	69.4518	129.2586	66.7249	125.6594	61.8635	120.6687
6	72.5960	132.7934	69.5804	128.8327	64.1827	123.3880
7	76.1170	136.8190	72.7759	132.4289	66.7803	126.4857
8	79.9546	141.2694	76.2551	136.3815	69.6073	129.9159
9	84.0562	146.0577	79.9677	140.6171	72.6283	133.6319
10	88.3764	150.9984	83.8699	145.0520	75.7998	137.5879

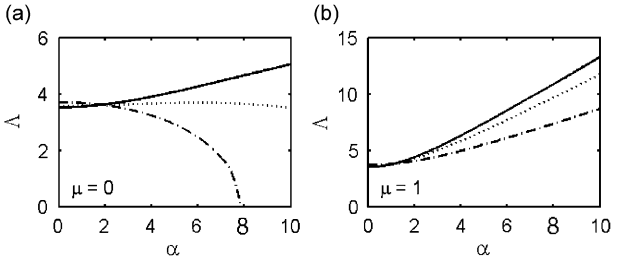

Fig. 3. Influence of arc angle θ_0 and rotational speed α on fundamental natural frequencies of straight and curved cantilever beams at (a) $\mu = 0$ and (b) $\mu = 1$ (β_v, $\beta_\theta \to \infty$; $L_z = 200$; (—) $\theta_0 = 0$, ($\cdots$) $\theta_0 = 50^\circ$, and (– · –) $\theta_0 = 90^\circ$).

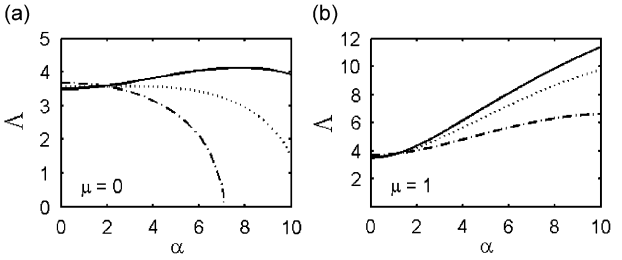

Fig. 4. Influence of arc angle θ_0 and rotational speed α on fundamental natural frequencies of straight and curved cantilever beams at (a) $\mu = 0$ and (b) $\mu = 1$ ($\beta_v = 1000$, $\beta_\theta \to \infty$; $L_z = 200$; (—) $\theta_0 = 0$, ($\cdots$) $\theta_0 = 50^\circ$, and (– · –) $\theta_0 = 90^\circ$).

that at a certain critical value of this coupled effect, the fundamental natural frequency reduces to zero, i.e. a divergent instability (tension buckling) condition occurs [27]. However, at higher vibrational modes, Tables 2(a) and (b) show that the coupled effect exerts less influence on the dynamic response of the beam. From inspection, it is found that the corresponding natural frequencies increase with increasing rotational speed, and decrease with increasing arc angle.

Table 3 illustrates the effect of the rotational speed and arc angle on the first four natural frequencies of a curved cantilever beam with a slenderness ratio $L_z = 100$ mounted in a hub with a radius of $\mu = 1$. Comparing Tables 2 and 3, it is evident that for a given value of the rotational speed, the natural frequencies associated with the first four vibrational modes of the rotating beam increase as the hub radius is increased. Furthermore, in direct contrast to the results presented in Table 2 for $\mu = 0$, it is observed that the hub radius effect causes

the first natural frequency to increase rather than decrease with increasing rotational speed at the highest arc angle of $\theta_0 = 90^\circ$.

Figs. 3–5 illustrate the effect of the translational spring constant β_v on the fundamental natural frequencies Λ_1 of straight and curved rotating beams. Note that rotational displacement at the root is not allowed, and thus $\beta_\theta \to \infty$ in every case. The three figures correspond to translational spring constants of ∞, 1000, and 100, respectively, and show that the spring constant has a significant effect on the fundamental natural frequencies of the two beams. Fig. 3(a) shows that in the case where the hub radius is $\mu = 0$, the fundamental natural frequency of the curved cantilever beam with an arc angle of 90° decreases as the rotational speed is increased. Furthermore, it can be seen that at a certain critical value of the rotational speed, a divergent instability condition occurs, i.e. the fundamental natural frequency falls to zero. However, Fig. 3(b) shows that the hub radius effect causes the fundamental natural frequency of the curved beam to increase with an increasing

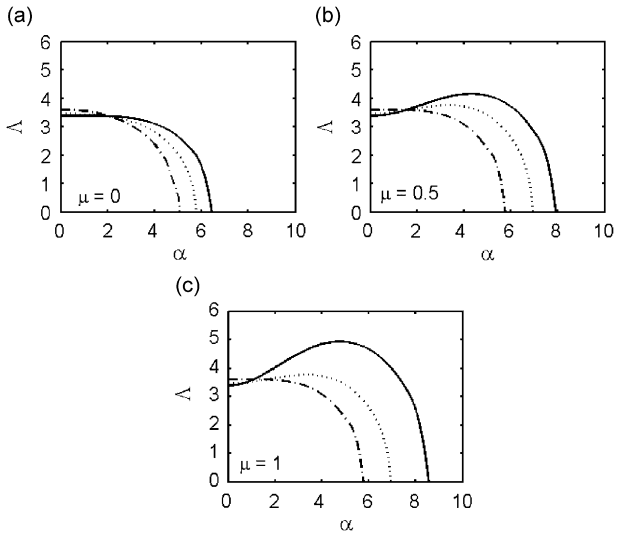

Fig. 5. Influence of arc angle θ_0 and rotational speed α on fundamental natural frequencies of straight and curved cantilever beams at (a) $\mu = 0$, (b) $\mu = 0.5$ and (c) $\mu = 1$ ($\beta_v = 100$, $\beta_\theta \to \infty$; $L_z = 200$; (—) $\theta_0 = 0$, (· · · ·) $\theta_0 = 50^\circ$, and (– · –) $\theta_0 = 90^\circ$).

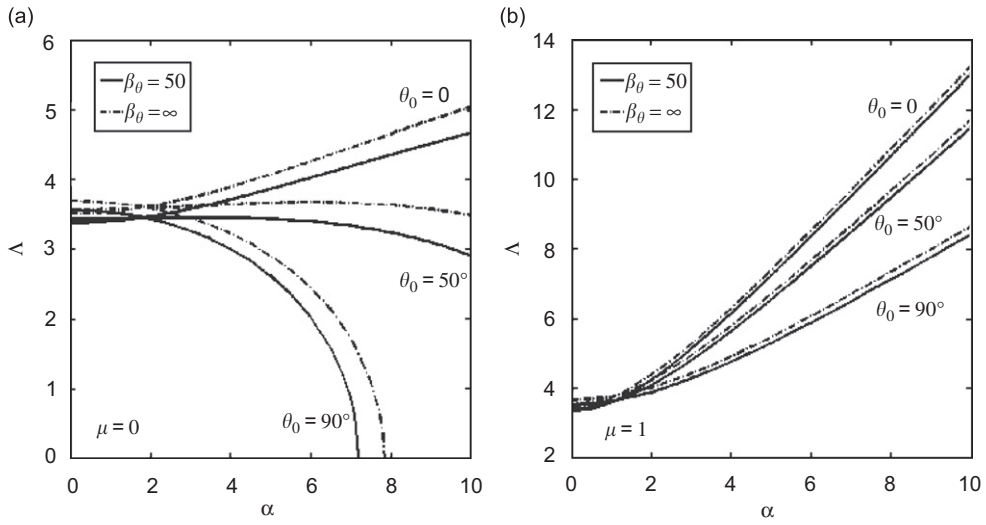

Fig. 6. Influence of arc angle θ_0 and rotational spring constant β_θ on fundamental natural frequencies of straight and curved cantilever beams at (a) $\mu = 0$ and (b) $\mu = 1$ ($\beta_\theta \to \infty$; $L_z = 200$).

rotational speed at all values of the arc angle, including $\theta_0 = 90^\circ$. When the translational spring constant β_v is reduced from infinity to a value of 1000, Fig. 4 shows that the fundamental natural frequencies decrease significantly at both values of the hub radius. Furthermore, it can be seen that as in Fig. 3(b), divergent instability does not occur when the hub radius is increased to $\mu = 1$. However, when the translational spring constant is reduced further to 100, it is seen that divergent instability occurs at all values of the arc angle and hub radius. Overall, the results presented in Figs. 3–5 reveal that the natural frequencies of the straight and curved beams decrease significantly with a decreasing translational spring constant β_v, with the result that at a certain critical value of β_v, divergent instability occurs irrespective of the hub radius value.

Fig. 6 illustrates the influence of the rotational spring constant β_θ on the fundamental natural frequencies Λ_1 of straight and curved rotating beams for the case where translation displacement at the root is not allowed, i.e. $\beta \to \infty$. It is observed that at all values of the arc angle and rotational speed, the natural frequency increases slightly with an increasing rotational spring constant, β_θ. Furthermore, comparing the results presented in Fig. 6 with those presented in Figs. 3–5, it is apparent that the degree of influence of the rotational spring constant β_θ on the natural frequency of the two beams is far lower than that of the translational spring constant β_v.

7. Conclusion

Utilizing Hamilton's principle and a consistent linearization approach, this study has established the governing differential equations and boundary conditions for the free vibration of a rotating curved beam with an elastically restrained root. Explicit relations have been derived to correlate the displacements of the beam in the axial and radial directions, respectively, and a closed-form solution of the general system has been obtained. The respective effects of the arc angle, the root spring constants, the rotational speed, and the hub radius on the natural frequencies and divergent instability characteristics of a curved rotating beam have been systematically examined and compared with those observed for a straight beam. The major findings of the present study can be summarized as follows:

(1) Given a sufficiently small value of the arc angle, the fundamental natural frequencies of a curved cantilever beam increase with an increasing rotational speed. However, at higher values of the arc angle and smaller values of the hub radius, the coupled effect of the arc angle and the rotational speed reduces the bending rigidity of the beam in the first vibrational mode. At a certain critical value of the coupled effect, the fundamental natural frequency reduces to zero, indicating the onset of a divergent instability condition.
(2) The natural frequencies of the curved beam increase with an increasing value of the hub radius.
(3) The natural frequencies of the curved beam also increase as the values of the translational and rotational spring constants are increased. Of the two spring constants, the translational spring constant has a significantly greater effect on the natural frequency of the beam.
(4) Given a sufficiently low value of the translational spring constant, a divergent instability effect is induced in the rotating curved beam even at large values of the hub radius.

Acknowledgement

The support of the National Science Council of Taiwan, ROC, is gratefully acknowledged (Grant no. NSC96-2218-E-218-001).

Appendix A

The coefficients of the displacement relations given in Eq. (25) are as follows:

$$k_1 = \frac{(\Lambda^2 + \alpha^2)^2}{\theta_0} + \frac{L_z^4(\Lambda^2 + \alpha^2)}{\theta_0} + \theta_0 L_z^2(\Lambda^2 + \alpha^2),$$

$$k_2 = -\left(3L_z^2 + \frac{L_z^4}{\theta_0^2} + \theta_0^2\right)(\Lambda^2 + \alpha^2) + \theta_0^2 L_z^2(\theta_0^2 + L_z^2),$$

$$k_3 = -\alpha^2\left(\theta_0^2 + 2L_z^2 + \frac{L_z^4}{\theta_0^2}\right), \quad k_4 = (2\theta_0^2 L_z^2 + 2L_z^4 + \Lambda^2 + \alpha^2),$$

$$k_5 = \left(L_z^2 + \frac{L_z^4}{\theta_0^2}\right), \quad k_6 = \theta_0^2 L_z^2 + L_z^4 + \Lambda^2 + \alpha^2,$$

$$k_7 = (\Lambda^2 + \alpha^2)\left(\theta_0 + \frac{L_z^2}{\theta_0}\right) - \theta_0 L_z^2(\theta_0^2 + L_z^2), \quad k_8 = \alpha^2\left(\theta_0 + \frac{L_z^2}{\theta_0}\right).$$

Appendix B

The coefficients of the boundary conditions given in Eqs. (28) and (29) are as follows:

$b_{11} = 0,$

$b_{12} = k_2 + k_3\bar{N}_p''(0),$

$b_{13} = 2k_3\bar{N}_p'(0),$ fc

$b_{14} = k_3\bar{N}_p(0) + k_4,$

$b_{15} = 0,$

$b_{16} = k_5,$

$b_{21} = \beta_v,$

$b_{22} = -\alpha^2\bar{N}_p(0) - \frac{k_2k_8\theta_0}{k_3k_6} - \frac{k_8\theta_0}{k_6}\bar{N}_p''(0) - \frac{k_8\theta_0L_z^2}{k_3},$

$b_{23} = -\frac{2k_8\theta_0}{k_6}\bar{N}_p'(0),$

$b_{24} = 1 + \frac{k_8\theta_0}{k_3} - \frac{k_8\theta_0}{k_6}\bar{N}_p(0) - \frac{k_4k_8\theta_0}{k_3k_6},$

$b_{25} = 0,$

$b_{26} = -\frac{k_5k_8\theta_0}{k_3k_6},$

$b_{31} = -\frac{k_7\theta_0}{k_6},$

$b_{32} = -\beta_\theta - \frac{k_8\theta_0}{k_6}\bar{N}_p'(0) + \frac{k_2\theta_0\beta_\theta}{k_1} + \frac{k_3\theta_0\beta_\theta}{k_1}\bar{N}_p''(0),$

$b_{33} = 1 - \frac{k_8\theta_0}{k_6}\bar{N}_p(0) + \frac{2k_3\theta_0\beta_\theta}{k_1}\bar{N}_p'(0) + \frac{\theta_0^2L_z^2}{k_6},$

$b_{34} = \frac{k_3\theta_0\beta_\theta}{k_1}\bar{N}_p(0) + \frac{k_4\theta_0\beta_\theta}{k_1},$

$b_{35} = \frac{L_z^2}{k_6},$

$b_{36} = \frac{k_5\theta_0\beta_\theta}{k_1},$

$b_{41} = \theta_0 + \frac{k_7}{k_6},$

$b_{42} = \frac{k_8}{k_6}\bar{N}_p'(1),$

$b_{43} = -\frac{\theta_0L_z^2}{k_6},$

$b_{44} = 0,$

$b_{45} = -\frac{L_z^2}{k_6\theta_0},$

$b_{46} = 0,$

$b_{51} = 0,$

$b_{52} = -\frac{k_2k_8\theta_0}{k_3k_6} - \frac{k_8\theta_0}{k_6}\bar{N}_p''(1) - \frac{k_8\theta_0L_z^2}{k_3},$

$b_{53} = -\frac{2k_8\theta_0}{k_6}\bar{N}_p'(1),$

$b_{54} = 1 + \frac{k_8\theta_0}{k_3} - \frac{k_4k_8\theta_0}{k_3k_6},$

$b_{55} = 0,$

$b_{56} = -\frac{k_5k_8\theta_0}{k_3k_6},$

$b_{61} = -\frac{k_7\theta_0}{k_6},$

$b_{62} = -\frac{k_8\theta_0}{k_6}\bar{N}_p'(1),$

$b_{63} = 1 + \frac{\theta_0^2L_z^2}{k_6},$

$b_{64} = 0,$

$b_{65} = \frac{L_z^2}{k_6},$

$b_{66} = 0.$

Appendix C

The process of reducing the boundary conditions given in Eqs. (28) and (29) for a curved beam to those given in Eqs. (41) and (42) for a straight beam can be summarized as follows:

Write the relations given in Eq. (25) in the form

$$\theta_0 \bar{U} = \frac{L_z^4}{(\Lambda^2+\alpha^2)^2+(\Lambda^2+\alpha^2+L_z^4)} \frac{\partial}{\partial\xi}[\bar{V}^{(4)} - \alpha^2(\bar{N}_p\bar{V}')' - (\Lambda^2+\alpha^2)\bar{V}],$$

$$\theta_0 \bar{U}' = -\frac{L_z^2}{(\Lambda^2+\alpha^2+L_z^4)}[\bar{V}^{(4)} - \alpha^2(\bar{N}_p\bar{V}')' - (\Lambda^2+\alpha^2)\bar{V}],$$

$$\theta_0 \bar{U}'' = \frac{L_z^2}{(\Lambda^2+\alpha^2+L_z^4)} \frac{\partial}{\partial\xi}[\bar{V}^{(4)} - \alpha^2(\bar{N}_p\bar{V}')' - (\Lambda^2+\alpha^2)\bar{V}]. \tag{C.1}$$

Specifying $\theta_0 = 0$ in the above relations yields

$$\frac{\partial}{\partial\xi}[\bar{V}^{(4)} - \alpha^2(\bar{N}_p\bar{V}')' - (\Lambda^2+\alpha^2)\bar{V}] = 0, \quad \bar{V}^{(4)} - \alpha^2(\bar{N}_p\bar{V}')' - (\Lambda^2+\alpha^2)\bar{V} = 0,$$

$$\frac{\partial}{\partial\xi}[\bar{V}^{(4)} - \alpha^2(\bar{N}_p\bar{V}')' - (\Lambda^2+\alpha^2)\bar{V}] = 0. \tag{C.2}$$

Substituting the relations given in Eq. (C.2) into the boundary conditions given in Eqs. (28) and (29) yields the limiting boundary conditions given in Eqs. (41) and (42).

References

[1] A. Leissa, Vibrational aspects of rotating turbomachinery blades, *ASME Applied Mechanics Reviews* 34 (1981) 629–635.

[2] V. Ramamurti, P. Balasubramanian, Analysis of turbomachine blades: a review, *The Shock and Vibration Digest* 16 (1984) 13–28.

[3] J.S. Rao, Turbomachine blade vibration, *The Shock and Vibration Digest* 19 (1987) 3–10.

[4] S.M. Lin, J.F. Lee, S.Y. Lee, W.R. Wang, Prediction of vibration of rotating damped beams with arbitrary pretwist, *International Journal of Mechanical Sciences* 48 (2006) 1494–1504.

[5] C.L. Ko, Dynamic analysis for free vibrations of rotating sandwich tapered beams, *AIAA Journal* 27 (3) (1989) 359–369.

[6] J.S. Tomar, Thermal effect on frequencies of coupled vibrations of pretwisted rotating beams, *AIAA Journal* 23 (8) (1985) 1293–1296.

[7] V.T. Nagaraj, P. Shanthakumar, Rotor blade vibrations by the Galerkin finite element method, *Journal of Sound and Vibration* 43 (1975) 575–577.

[8] D.H. Hodges, M.J. Rutkowski, Free-vibration analysis of rotating beams by a variable-order finite element method, *AIAA Journal* 19 (11) (1981) 1459–1466.

[9] T.H. Young, T.M. Lin, Stability of rotating pretwisted, tapered beams with randomly varying speeds, *ASME Journal of Vibration and Acoustics* 120 (3) (1998) 784–790.

[10] S.M. Hashemi, M.J. Richard, G. Dhatt, A new dynamic finite element(DFE) formulation for lateral free vibration of Euler–Bernoulli spinning beams using trigonometric shape functions, *Journal of Sound and Vibration* 220 (1999) 601–624.

[11] J.R. Banerjee, Free vibration of centrifugally stiffened uniform and tapered beams using the dynamic stiffness method, *Journal of Sound and Vibration* 233 (5) (2000) 857–875.

[12] D. Storti, Y. Aboelnaga, Bending vibrations of a class of rotating beams with hypergeometric solutions, *ASME Journal of Applied Mechanics* 54 (2) (1987) 311–314.

[13] S.Y. Lee, Y.H. Kuo, Bending vibrations of a rotating nonuniform beam with an elastically restrained root, *Journal of Sound and Vibration* 154 (3) (1992) 441–451.

[14] S.Y. Lee, Y.H. Kuo, Exact solutions for the analysis of general elastically restrained nonuniform beams, *ASME Journal of Applied Mechanics* 59 (1992) 205–212.

[15] S.Y. Lee, S.M. Lin, Bending vibrations of rotating nonuniform Timoshenko beams with an elastically restrained root, *ASME Journal of Applied Mechanics* 61 (4) (1994) 949–955.

[16] S.M. Lin, S.Y. Lee, W.R. Wang, Dynamic analysis of rotating damped beams with an elastically restrained root, *International Journal of Mechanical Sciences* 46 (2004) 673–693.

[17] M.G. Beiler, T.H. Carolus, Computation and measurement of the flow in axial flow fans with skewed blades, *ASME Journal of Turbomachinery* 121 (1999) 59–66.

[18] J.T.S. Wang, O. Mahrenholtz, Bending frequencies of a rotating curved beam, *Ingenieur-Archiv* 44 (1975) 399–407.

[19] J.H. Park, J.H. Kim, Dynamic analysis of rotating curved beam with a tip mass, *Journal of Sound and Vibration* 228 (5) (1999) 1017–1034.

[20] G.R. Heppler, J.S. Hansen, Timoshenko beam finite element using trigonometric basis functions, *AIAA Journal* 26 (1988) 1378–1386.

[21] J.C. Simo, L.V. Quoc, The role of non-linear theories in transient dynamic analysis of flexible structures, *Journal of Sound and Vibration* 119 (1987) 487–508.
[22] J. Henrych, *The Dynamics of Arches and Frames*, Elsevier, New York, 1981.
[23] R.O. Stafford, V. Giurgiutiu, Semi-analytic methods for rotating Timoshenko beams, *Journal of Mechanical Sciences* 17 (1975) 719–727.
[24] V. Giurgiutiu, R.O. Stafford, *Semi-analytic Methods for Frequencies and Mode-shapes of Rotor Blades, Vertica*, Vol. 1, Pergamon Press, Oxford, 1977, pp. 291–306.
[25] H.H. Yoo, S.H. Shin, Vibration analysis of rotating cantilever beams, *Journal of Sound and Vibration* 212 (1998) 807–828.
[26] S. Putter, H. Mandor, Natural frequencies of radial rotating beams, *Journal of Sound and Vibration* 56 (1978) 175–185.
[27] S.M. Lin, S.Y. Lee, Prediction of vibration and instability of rotating damped beams with an elastically restrained root, *International Journal of Mechanical Science* 46 (2004) 1173–1194.